

A Pipeline for ADNI Resting-State Functional MRI Processing and Quality Control

Saige Rutherford¹, Zeshawn Zahid¹, Robert C. Welsh², Andrea Avena-Koenigsberger³,
Vincent Koppelmans⁴, Amanda F. Mejia¹

¹Department of Statistics, Indiana University, Bloomington, USA

²Psychiatry and Biobehavioral Sciences, University of California, Los Angeles, USA

³Center for Neuroimaging, Indiana University School of Medicine, Bloomington, USA

⁴Department of Psychiatry, University of Utah, Salt Lake City, USA

Abstract

The Alzheimer's Disease Neuroimaging Initiative (ADNI) provides a comprehensive multimodal neuroimaging resource for studying aging and Alzheimer's disease (AD). Since its second wave, the ADNI has increasingly collected resting-state functional MRI (rs-fMRI), a valuable resource for discovering brain connectivity changes predictive of cognitive decline and AD. A major barrier to its use is the considerable variability in acquisition protocols and data quality, compounded by missing imaging sessions and inconsistencies in how functional scans temporally align with clinical assessments. As a result, many studies only utilize a small subset of the total rs-fMRI data, limiting statistical power, reproducibility, and the ability to study longitudinal functional brain changes at scale. Here, we describe a pipeline for ADNI rs-fMRI data that encompasses the download of necessary imaging and clinical data, temporally aligning the clinical and imaging data, preprocessing, and quality control. We integrate data curation and preprocessing across all ADNI sites and scanner types using a combination of open-source software (Clinica, fMRIprep, and MRIQC) and bespoke tools. Quality metrics and reports are generated for each subject and session to facilitate rigorous data screening. All scripts and configuration files are available to enable reproducibility. The pipeline, which currently supports ADNI-GO, ADNI-2, and ADNI-3 data releases, outputs high-quality rs-fMRI time series data adhering to the BIDS-derivatives specification. This protocol provides a transparent and scalable framework for curating and utilizing ADNI fMRI data, empowering large-scale functional biomarker discovery and integrative multimodal analyses in Alzheimer's disease research.

1 Introduction

The Alzheimer's Disease Neuroimaging Initiative (ADNI) is a large multicenter consortium comprising more than 60 academic and clinical sites across the United States and Canada. Established to validate, compare, and standardize clinical trial measures and biomarkers for Alzheimer's disease research, ADNI collects longitudinal MRI, PET, clinical, cognitive, and biochemical data from healthy older adults, individuals with mild cognitive impairment (MCI), and patients with Alzheimer's disease (AD) (Weiner et al., 2025). The primary objectives of ADNI are to develop standards for acquiring longitudinal, multisite MRI and PET data, to develop an accessible repository of longitudinal neuroimaging data (measuring brain structure, function, and metabolism), clinical, cognitive, and biochemical data, and to develop methods to maximize power to determine treatment effects in clinical trials (Petersen et al., 2010). ADNI is an ongoing study that began in 2004 and has been collecting data continuously across its various phases (Table 1).

Table 1. Overview of the phases of ADNI and the primary goal, timeline/duration, funding, and cohort description of each phase. Each cohort after ADNI 1 includes the previous cohort(s). This table was recreated from ADNI's website ("Alzheimer's Disease Neuroimaging Initiative," n.d.).

	ADNI 1	ADNI GO	ADNI 2	ADNI 3	ADNI 4
Timeline (duration)	2004-2010 (5 years)	2009-2011 (2 years)	2011-2016 (5 years)	2016-2022 (5 years)	2022-2027 (5 years)
Primary Goal	To develop biomarkers as outcome measures for clinical trials.	Examine biomarkers in earlier stages of disease.	Develop biomarkers as predictors of cognitive decline, and as outcome measures.	Study the use of tau PET and functional imaging techniques in clinical trials.	Improve generalizability of AD research.
Cohort	200 cognitively unimpaired (CU), 400 MCI, 200 AD	New: 200 early MCI	New: 150 CU, 150 elderly MCI, 150 late MCI, 150 AD	New: 133 CU, 151 MCI, 87 AD	New: 200 CU, 200 MCI, 100 AD/DEM

ADNI has been instrumental in advancing understanding of neurodegeneration by providing large-scale, longitudinal neuroimaging and biomarker data across the spectrum of cognitive aging and dementia (Weiner et al., 2012, 2013, 2015, 2024; Yao et al., 2017). There has been broad and sustained use of ADNI data in structural and PET imaging

studies. A recent paper estimated there are more than 5,500 publications, 30,000 data use agreements, and 405 million image downloads utilizing ADNI data (Toga et al., 2024).

In contrast, a targeted PubMed search for publications using ADNI resting-state functional MRI (rs-fMRI) data (using the terms “ADNI” OR “Alzheimer’s Disease Neuroimaging Initiative” AND “fMRI” OR “functional MRI” OR “rsfMRI” OR “resting state”) identified only 152 publications as of November 2025 (Figure 1). A full list of these papers is provided in the supplement (Supplemental File 1). Although rs-fMRI data collection began five years later than structural MRI (in ADNI-GO, 2009, versus ADNI-1, 2004), this delay does not explain the disparity in use. Rather, rs-fMRI data are inherently more complex, require substantially more preprocessing, and are more sensitive to acquisition and quality-control issues, which have historically limited their accessibility to the broader research community. At the same time, this relative underutilization highlights a major opportunity: ADNI rs-fMRI represents a rich, longitudinal, and largely untapped resource for studying functional brain changes in aging and Alzheimer’s disease, particularly as preprocessing tools, standards, and computational resources continue to mature. *This imbalance contrasts with the central role of functional connectivity in contemporary models of neurodegeneration and highlights a structural barrier to reuse, rather than a lack of scientific relevance of rs-fMRI itself.*

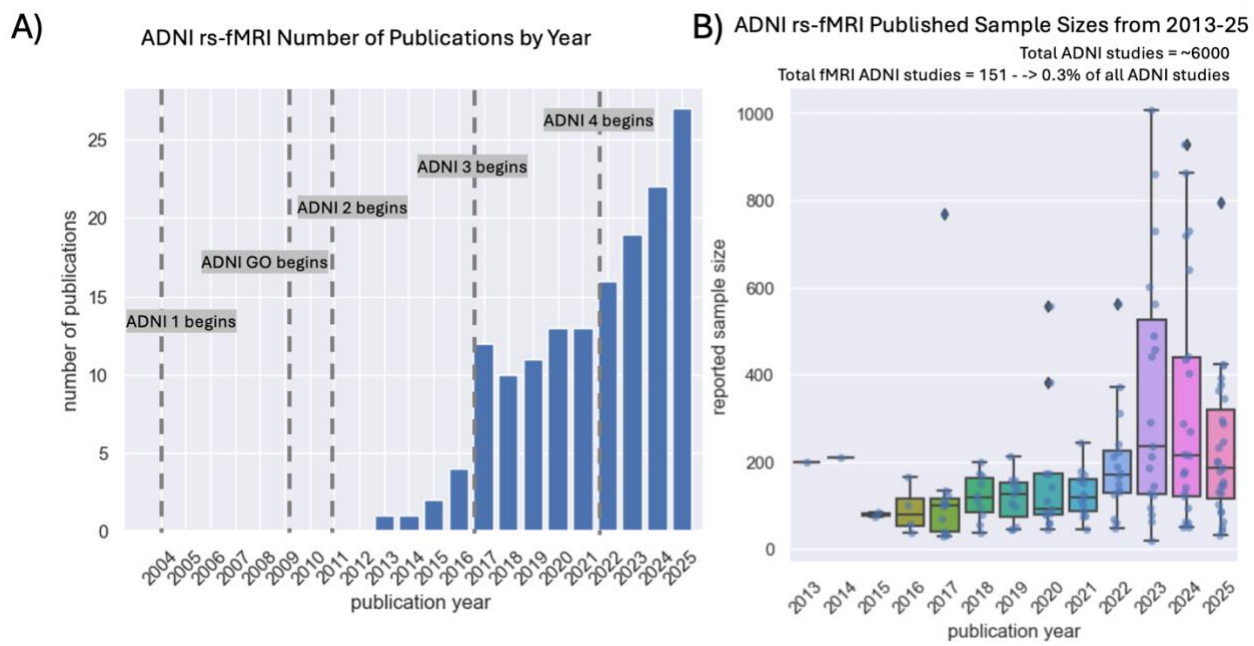


Figure 1. A) The number of published papers using ADNI rs-fMRI data per year (2013-Nov 2025). **B)** The reported sample sizes in each publication using ADNI rs-fMRI data, per year (2013-Nov 2025).

Reproducible neuroimaging research requires transparent documentation of the procedures used to access, preprocess, and quality control the data (Gau et al., 2021; Nichols et al., 2017). A unified, openly described fMRI preprocessing protocol for ADNI will accelerate large-scale secondary analyses of ADNI fMRI data. In this work, we describe a protocol that converts ADNI functional and structural MRI data into the Brain Imaging Data Structure (BIDS) format (K. J. Gorgolewski et al., 2016), applies standardized preprocessing, performs quality assessment, identifies data requiring troubleshooting, and integrates clinical data. The pipeline combines established neuroimaging tools -- Clinica (Routier et al., 2021; Samper-González et al., 2018) for DICOM to NIFTI conversions and BIDSification, fMRIPrep (Esteban, Markiewicz, et al., 2018) for preprocessing and MRIQC (Esteban et al., 2017) for quality evaluation, and bespoke tools within an optional reproducible container environment, ensuring consistent outputs across computing systems.

By sharing all configuration files and processing scripts, we provide a complete blueprint for reproducing our ADNI fMRI data curation and preprocessing pipeline under the constraints of the ADNI data-use agreement. This resource supports transparent data preparation for subsequent biomarker discovery in Alzheimer's disease and related neurodegenerative conditions. While the protocol necessarily includes technical details, its primary contribution is to enable broad reuse of ADNI rs-fMRI data by the neuroscience and Alzheimer's disease research communities.

2 Methods

This section describes the complete ADNI resting-state fMRI data preparation pipeline, organized according to the eight main workflow steps (Figure 2) implemented in the accompanying public GitHub repository (https://github.com/mandymejia/ADNI_fMRI_protocol). For each step, we specify the data inputs, processing operations, software tools and versions, quality-control procedures, and known issues specific to ADNI. All scripts, container specifications, configuration files, and workflow orchestration tools referenced below are available in the repository. This pipeline currently supports ADNI-GO, ADNI-2, and ADNI-3 datasets.

A) Visual Overview B) Flowchart of steps C) GitHub Directory

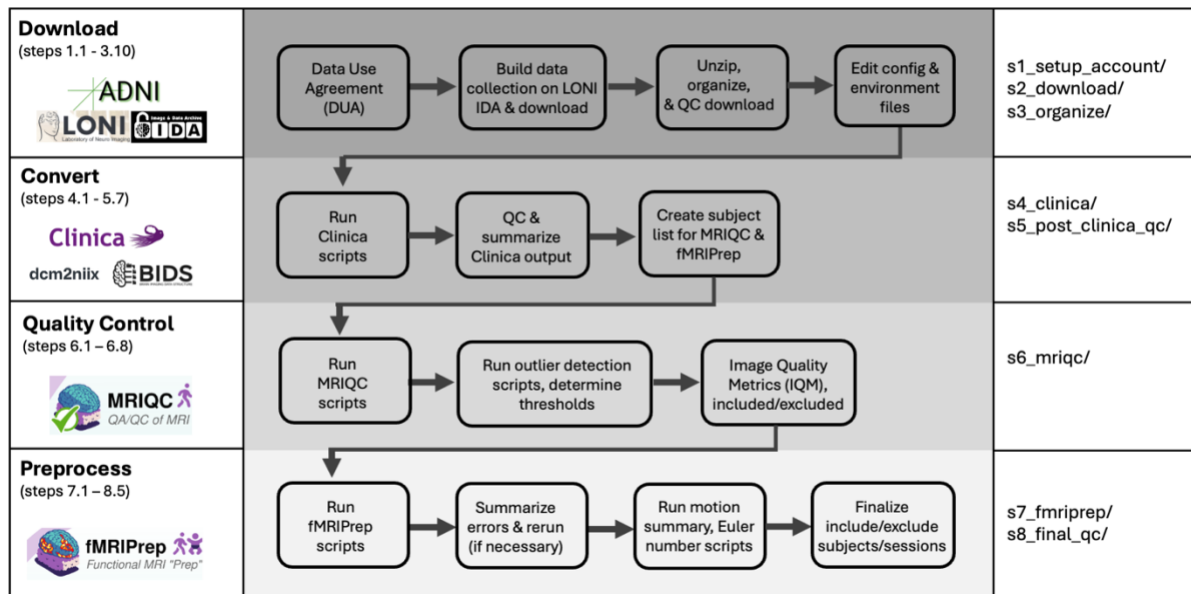


Figure 2. Overview of all steps in our ADNI fMRI data curation pipeline. The step numbers listed in this figure correspond to the detailed steps in the supplemental file (pipeline instructions PDF) and in the GitHub repository (https://github.com/mandymejia/ADNI_fMRI_protocol).

2.1 Step 1: Account Setup and Data-Use Agreement

Raw imaging and clinical data are accessed through the Laboratory of Neuro Imaging Image and Data Archive (LONI/IDA) (<https://ida.loni.usc.edu>) after account registration and approval of ADNI’s Data Use Agreement (DUA) (<https://ida.loni.usc.edu/collaboration/access/appLicense.jsp>). The protocols here provide detailed instructions (further detailed instructions are available in s1_setup_account/) for users to reproduce the entire workflow independently; however, no raw data are shared via our repository, in compliance with ADNI’s DUA. All processing is performed within secure institutional or high-performance computing (HPC) environments, consistent with ADNI DUA requirements.

2.2 Step 2: Data Selection and Download from LONI

The second step involves selecting eligible ADNI sessions and downloading the associated imaging files, metadata spreadsheets, and study information packages (further instructions in s2_download/). Using the “Image Collections” tool in LONI/IDA, users can filter for resting-state fMRI sequences and associated structural sequences (T1 & T2) across the ADNI-GO, ADNI-2, and ADNI-3 phases. ADNI-1 is excluded because it does not

include resting-state fMRI, and Clinica does not yet support ADNI-4. The GitHub repository for the pipeline includes step-by-step screenshots and instructions for building reproducible LONI queries. All downloaded ZIP files, including raw imaging archives (DICOM format), metadata spreadsheets (e.g., ADNIMERGE.csv, MPRAGEMETA.csv, MRILIST.csv, scanner QC tables), and ADNI study files (clinical/behavioral data, protocol descriptions, acquisition parameters), should be stored as defined in the user's configuration file. For the current manuscript, data up to October 1st, 2025, were downloaded and used for the development and testing of the pipeline.

2.3 Step 3: DICOM Organization and Integrity Checks

After download, all ZIP archives are uncompressed, reorganized into a standardized directory structure, and subjected to basic data quality checks. Scripts in s3_organize/ verify the DICOM download (expected number of directories based on image collection) and map the heterogeneous DICOM directory names to their corresponding imaging modalities (i.e., T1, T2, fMRI (i.e., BOLD)).

2.4 Step 4: Imaging and Clinical Data Conversion Using Clinica

DICOM-to-BIDS Image Conversion

DICOM files are converted into the Brain Imaging Data Structure (BIDS; v1.10.1) (K. J. Gorgolewski et al., 2016) format using Clinica (v0.10.1) (Routier et al., 2021; Samper-González et al., 2018). The command-line interface and configuration parameters are provided in s4_clinica/. Clinica serves three main functions: i) DICOM to NIfTI conversion and metadata extraction (via dcm2niix), ii) automated matching of imaging sessions to clinical visits, and iii) organizing data into BIDS format. Clinica cross-references session dates using several ADNI spreadsheets (e.g., ADNIMERGE, MPRAGEMETA, and quality-control tables) to ensure accurate mapping of T1, T2, and BOLD series to visit codes. After conversion, the resulting dataset is validated using the BIDS Validator (v1.14.7). Each participant's BIDS dataset contains both structural (T1 and, if available, T2) and functional (BOLD) images, along with all required metadata fields necessary for downstream processing with fMRIprep and MRIQC.

During the development of this protocol, we identified several issues in the ADNI DICOMs that must be addressed. These include items identified by Clinica (interslice distance variation and failed image conversion, both documented in s4_clinica/known_clinica_DICOM_errors.csv) and several errors we encountered that were not reported by Clinica (missing or incorrect PhaseEncodingDirection parameter, missing

JSON sidecar files for T1 files, and T1 DICOM conversion errors). Our scripts automatically flag these issues (s5_post_clinica_qc/analysis/create_report/run_session_heuristics.py & main.ipynb). Subjects with unrecoverable errors are excluded at this stage (i.e., failed image conversion).

Matching Imaging Sessions to Clinical Data

Data that do not change over time (e.g., sex, education level, or diagnosis at baseline), are pulled from the ADNIMERGE file and put in the participants.tsv file, located at the top of the BIDS folder hierarchy. The time-varying data (e.g., the clinical scores) are pulled from specific CSV files (e.g., MMSE.csv) and put in participant-id_session-id.tsv files in each participant subfolder. The clinical data being converted (i.e., temporally aligned with the imaging visits) are defined in a spreadsheet (clinical_specifications_adni.xlsx) that is available with the Clinica codebase. It is possible to modify this file if additional clinical data should be converted. For a more detailed description of Clinica, including some of the decisions about which scan to select (e.g., if there are multiple T1 per session), we refer readers to their detailed documentation

(<https://aramislab.paris.inria.fr/clinica/docs/public/dev/Converters/ADNI2BIDS/>) and user support Google group (<https://groups.google.com/g/clinica-user>).

2.5 Step 5: Post-Clinica Data Quality Checks

After DICOM and BIDS conversion, additional QC steps ensure that each session meets minimum functional and structural imaging criteria (s5_post_clinica_qc/). Five heuristics regarding the scanner parameters are applied (Table 2). These heuristics were determined by an expert in MR physics (author RCW) and were chosen to detect errors in the data that occurred during collection. All scanner parameters were reviewed across sites/scanners to aid in the heuristic threshold choices. A notebook (s5_post_clinica_qc/analysis/create_report/main.ipynb) creates per-site and per scanner manufacturer (i.e., Siemens, GE, Philips) QC plots as well as the summary tables of scanner parameters and inclusion/exclusion sample sizes at each decision point. This notebook also summarizes and categorizes Clinica output errors. The final step of this notebook is to export a CSV file with the subjects and sessions to be passed on to MRIQC and fMRIPrep. This notebook is also available as a Python script (s5_post_clinica_qc/analysis/create_report/run_session_heuristics.py) to help with reproducibility and automation.

Table 2. Heuristics for excluding subjects/sessions based on scanner parameters.

Metric	Exclusion Rule	Rationale
ScanDepth = $\text{dim}_3 \times \text{pixdim}_3$	Outside range [155, 180]	Ensures adequate brain coverage
Repetition Time (TR)	Outside [0.5–1.0] or [2.9–3.1] seconds	Detects mislabeled scans or protocol inconsistencies
Minimum total scan duration	< 300 seconds	Ensures ≥5 minutes of fMRI data
PercentPhaseFOV	< 72	Indicates spatial under sampling
CoilString	Q-Body or BODY coils	Nonstandard or problematic coils

2.6 Step 6: Automated QC Metrics and Outlier Detection with MRIQC

MRIQC (v23.1.0) (Esteban et al., 2017) is run using scripts in s6_mriqc/. Sixteen automated participant-level image quality metrics (IQMs) are generated by MRIQC for each individual session, and group-level summaries are used to define quantitative exclusion criteria.

Automated IQM Outlier Detection

There are no established thresholds for these IQMs to our knowledge. To determine cutoffs for these IQMs in an automated fashion, we use an outlier-detection method developed in our lab (Parlak et al., 2025). For each IQM, the distribution across sessions is transformed to approximately follow a Normal distribution using a statistically robust, flexible transformation to eliminate skew and heavy or light tails. In the standard Normal distribution, values beyond ± 4 are extremely unlikely ($p < 0.000063$). Thus, after transformation, values above 4 or below -4 (depending on whether higher or lower values of the IQM are considered better, see Table 3) are flagged. These cutoffs are translated back to the original scale of the data by applying the reverse transformation.

We visualize the distribution of the IQMs for structural and functional data in Figures 3 and 4, along with the thresholds for exclusion. Examples of excluded subjects for each metric are shown in the supplemental figures. We also visualize these metrics per site in the supplement. An image was classified as failed if *any* IQM exceeded its threshold. If the T1 image was flagged as an outlier, the BOLD image was also excluded because the BOLD cannot be successfully preprocessed without a high-quality T1 image from the same session. This approach offers a reproducible and interpretable strategy for identifying problematic scans in heterogeneous, multicenter datasets. The full list of IQMs is provided in Table 3, and the code implementing this procedure (and for visualizations) is included in s6_mriqc/outlier_mriqc.R.

Table 3. Automated image quality metrics from MRIQC.

Name	Used for	Description	Direction
Contrast to Noise Ratio (CNR) (Magnotta et al., 2006)	T1	Extension of the SNR to evaluate how separated the tissue distributions of GM and WM are.	Higher = better
Signal to Noise Ratio (SNR) (Kaufman et al., 1989)	T1	The mean intensity within gray matter divided by the standard deviation of the values outside the brain.	Higher = better
Tissue probability overlap map (TPM) of Cerebrospinal Fluid (CSF)	T1	Overlap estimated from the CSF image and the corresponding maps from the ICBM nonlinear-asymmetric 2009c template.	Higher = better
TPM of Gray Matter (GM)	T1	Overlap estimated from the GM image and the corresponding maps from the ICBM nonlinear-asymmetric 2009c template.	Higher = better
TPM of White Matter (WM)	T1	Overlap estimated from the WM image and the corresponding maps from the ICBM nonlinear-asymmetric 2009c template.	Higher = better
Coefficient of Joint Variation (CJV) (Ganzetti et al., 2016)	T1	CJV of GM and WM: objective function for the optimization of INU correction algorithms. Higher values are related to the presence of heavy head motion and large INU artifacts.	Lower = better
Entropy Focus Criterion (EFC) (Atkinson et al., 1997)	T1	Uses the Shannon entropy of voxel intensities as an indication of ghosting and blurring induced by head motion.	Lower = better
Full Width Half Max (FWHM (mm)) (Friedman et al., 2008)	T1	The FWHM of the spatial distribution of the image intensity values in units of voxels.	Lower = better
Signal to Noise Ratio (SNR) (Kaufman et al., 1989)	BOLD	The mean intensity within gray matter divided by the standard deviation of the values outside the brain.	Higher = better
Temporal Signal to Noise Ratio (TSNR)	BOLD	Median value of the tSNR map (average BOLD signal / temporal standard deviation).	Higher = better
AFNI's mean quality index (AQI) (Cox, 1996)	BOLD	Mean quality index as computed by AFNI's 3dTqual for each volume, it is one minus the Spearman's rank correlation of that volume with the median volume.	Lower = better
AFNI's outlier ratio (AOR) (Cox, 1996)	BOLD	Mean fraction of outliers per fMRI volume as given by AFNI's 3dToutcount.	Lower = better
Entropy Focus Criterion (EFC) (Atkinson et al., 1997)	BOLD	Uses the Shannon entropy of voxel intensities as an indication of ghosting and blurring induced by head motion.	Lower = better
Framewise displacement (meanFD) (Power et al., 2014)	BOLD	Expresses instantaneous head-motion. Rotational displacements are calculated as the displacement on the surface of a sphere of radius 50 mm.	Lower = better
Full Width Half Max (FWHM (mm)) (Friedman et al., 2008)	BOLD	The FWHM of the spatial distribution of the image intensity values in units of voxels.	Lower = better
Temporal derivative of RMS variance over voxels (DVARS) (Power et al., 2012)	BOLD	Indexes the rate of change of BOLD signal across the entire brain at each frame of data.	Lower = better

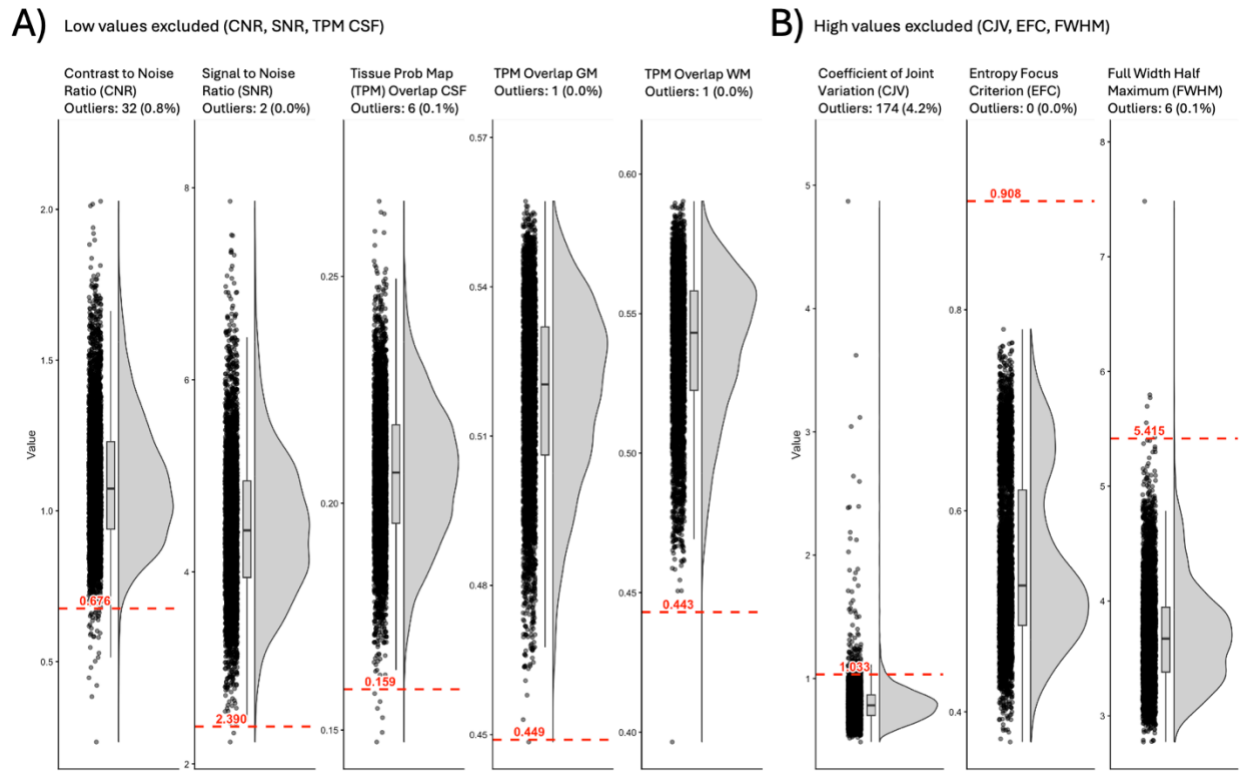


Figure 3. MRIQC Image Quality Metrics (IQMs) for structural (T1) images. These metrics are explained in Table 3. The red line indicates the outlier threshold. A) images below this line are excluded, and B) images above this line are excluded. Subjects were excluded if they had an outlier on any of these.

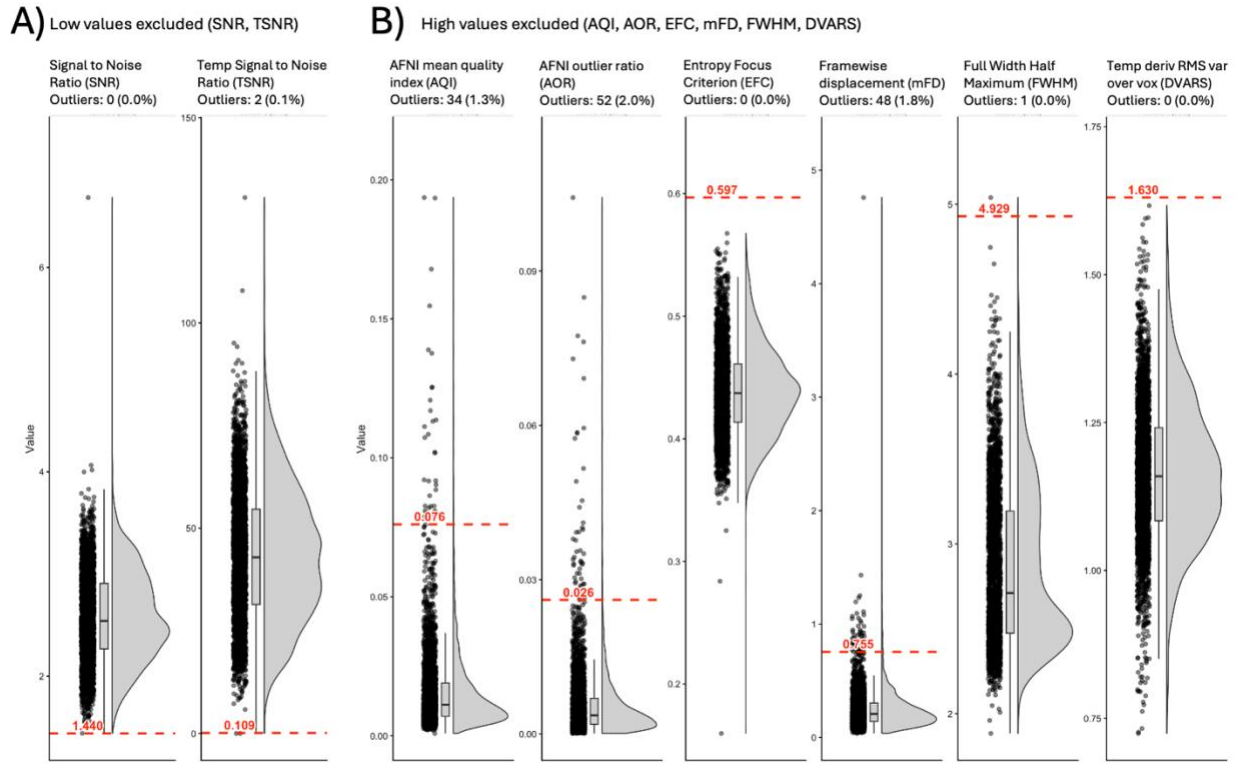


Figure 4. MRIQC Image Quality Metrics (IQMs) for BOLD images. These metrics are explained in Table 3. The red line indicates the outlier threshold. A) images below this line are excluded, and B) images above this line are excluded. Sessions were excluded if they had an outlier on any of these.

2.7) Step 7: fMRIPrep Preprocessing

Image preprocessing is performed using containerized execution (Apptainer v1.3.6) and fMRIPrep version 25.2.3 (Esteban, Blair, et al., 2018; Esteban, Markiewicz, et al., 2018), which is based on Nipype 1.10.0 (K. Gorgolewski et al., 2011; K. J. Gorgolewski et al., 2018). Many internal operations of fMRIPrep use Nilearn 0.11.1 (Abraham et al., 2014), mostly within the functional processing workflow. For more details of the pipeline, see the section corresponding to workflows in fMRIPrep's documentation (<https://fmriprep.org/en/stable/>) and citation boilerplate (<https://www.nipreps.org/intro/transparency/#citation-boilerplates>). The scripts for this step and further instructions are in the directory `s7_fmriprep/`.

ADNI-specific fMRI preprocessing considerations

During the development of this protocol, we systematically analyzed fMRIPrep failures to improve the robustness and automation of the preprocessing workflow. We parse fMRIPrep log files (`s7_fmriprep/fmriprep_error_report.py`) and explore and categorize error types in an accompanying notebook (`s7_fmriprep/explore_fmriprep_errors.ipynb`).

This analysis informed the design of upstream validation checks and conditional execution logic that ensure fMRIPrep jobs are only submitted when required inputs are present and preprocessing can complete successfully. Identified error categories include: i) missing BOLD files, ii) TemplateFlow cache/bind issues, iii) insufficient memory resources, iv) FreeSurfer recon-all failures, and v) fieldmap-less susceptibility distortion correction (syn-sdc) failures. For each category, the pipeline was designed to either automatically adapt execution parameters or skip processing and notify the user, depending on whether the error was recoverable. A more detailed description of these errors can be found in the supplement.

2.8 Step 8: Final QC and Derivation of the Analysis Sample

The last QC stage includes a final pass of quality checking the subjects and sessions that successfully completed fMRIPrep (and all previous steps). This includes summarizing the quality of the Freesurfer surface reconstruction using the Euler number (a measure of the topological complexity of the surface) and checking the functional runs for low motion. The Euler number has been shown to correlate highly with manual quality checking ratings (Rosen et al., 2018) and is the main metric used in automated QC methods (Klapwijk et al., 2019). Sessions with greater than 30% frames censored (with a framewise displacement threshold of 0.5 mm), and/or less than 5 minutes of low-motion data (after $FD > 0.5$ mm censoring) are excluded. This threshold can be adjusted by users if desired. A consolidated inclusion/exclusion table (with reasons coded per subject-session) is produced in `s8_final_qc/`. The final analysis-ready dataset includes all subjects meeting QC criteria across every stage of this protocol (DICOM download, Clinica DICOM to NIfTI conversion and BIDS formatting, MRIQC, and fMRIPrep preprocessing). Table 4 in Data Records reports the final number of subjects included/excluded at each step.

3 Data Records

The data records accompanying this protocol consist of (i) machine-readable quality-control summaries, (ii) pipeline logs and metadata, and (iii) versioned code and configuration files. These together allow any researcher with ADNI access to reproduce the dataset described here. The GitHub repository contains scripts, QC tables, and metadata. Researchers must obtain their own ADNI credentials to download the raw DICOMs and clinical data. All data records are organized according to the eight pipeline steps implemented in the GitHub repository and follow a structured flow from raw downloads to the final curated imaging dataset. Below, we describe the content and purpose of each record type, the associated GitHub folder or file, and the point in the pipeline at which each item is generated.

Overview of Dataset Flow

Table 4 provides a summary of the number of subjects and sessions at each stage of the pipeline, from download to final inclusion, based on our ADNI data download. This illustrates the cumulative effects of download issues, metadata inconsistencies, BIDS conversion failures, MRIQC-based outlier detection, preprocessing errors, and final quality thresholds on the resulting analysis sample.

Table 4. Inclusion and exclusion sample sizes at each step of the protocol. The Dropped column reports how many subjects (sub) and sessions (ses) were excluded from the previous step (row). The final column reports the sample size after exclusions up to each step. The sample consists of data from ADNI-GO, ADNI-2, and ADNI-3, the data releases used in our demonstration of the pipeline.

Pipeline Stage	GitHub Folder	Description	Dropped (Sub/Ses)	Subjects/ Sessions
Unzip & organize DICOMs	s3_organize/	Clean directory tree; check integrity	-	1153/2893
BIDS-convert via Clinica	s4_clinica/	NIfTI + JSON + sidecars	37/210	1116/2683
Post-Clinica QC	s5_post_clinica_qc/	TR/coverage/duration checks	11/62	1105/2621
MRIQC	s6_mriqc/	All IQMs present	12/12	1093/2611
Post-MRIQC QC	s6_mriqc/	Robust outlier detection	65/236	1028/2375
fMRIPrep	s7_fmriprep/	Volumetric, surface, grayordinates outputs	49/127	979/2248
Final QC passed	s8_final_qc/	Euler number, motion, ≥ 5 min usable data	66/202	913/2026

Reproducibility and Versioning of Data Records

All machine-readable outputs are automatically created by the pipeline and tracked through version control. The GitHub repository includes i) config/config_adni.yaml (a complete single-source-of-truth describing all paths, container versions, QC thresholds, and tool versions), ii) Makefile (defines the order and dependency structure of all steps), and iii) logs/ (Slurm logs, processing logs, and crash files). A Zenodo snapshot will archive the full repository with a DOI. Together, these records enable full reproduction of the curated dataset from raw ADNI data.

4 Technical Validation

The ADNI resting-state fMRI dataset is highly heterogeneous across scanner vendors, field strengths, study phases, and acquisition protocols. Rigorous technical validation is therefore essential to ensure data integrity and reproducibility. We conduct validation at every stage of the pipeline, closely aligned with the workflow described in the

Methods section (Figure 1). This validation comprises five major components: metadata validation and BIDS compliance, acquisition parameter validation, automated image quality evaluation, preprocessing integrity checks, and final inclusion validation.

Metadata Validation and BIDS Compliance (Clinica)

The first validation layer focuses on ensuring correctness and consistency of the converted dataset following DICOM-to-BIDS conversion via Clinica (Section 2.4). Failures at this stage, including malformed JSON sidecars, missing metadata fields, or directory inconsistencies, are flagged and excluded from downstream analysis. We review Clinica-generated outputs to identify conversion failures, mismatched session identifiers, and missing clinical metadata. Sessions affected by unrecoverable conversion errors are removed before further processing. All conversion decisions and failures are recorded in `s4_clinica/`.

Acquisition Parameter Validation (Post-Clinica QC)

To assess inter-site consistency and identify protocol anomalies, we summarize acquisition parameters across manufacturers, sites, and phases using the automated reports generated in `s5_post_clinica_qc/analysis/create_report/main.ipynb`. Validation at this stage explicitly targets ADNI-specific irregularities, including inconsistent repetition times (TR), incomplete brain coverage, nonstandard receiver coils, implausible scan durations, and under-sampled phase-encoding fields of view. Five scanner heuristics (Table 2) are applied uniformly across the dataset, based on expert review by an MR physicist (author RCW). Violations are logged and excluded before MRIQC and fMRIPrep. Figure 5 illustrates site- and manufacturer-level distributions of scanner parameters, while Figure 6 summarizes inclusion and exclusion counts at each QC stage. This validation step ensures that downstream quality control metrics reflect meaningful variation rather than acquisition parameter errors.

Automated Image Quality Validation (MRIQC)

Automated quality control is conducted using MRIQC (Section 2.6) for both structural (T1) and functional (BOLD) images. Sixteen image quality metrics (IQMs; Table 3) are output for every session. Outlier detection employs a robust, data-driven normalization framework developed in-house (Parlak et al., 2025). Summary distributions and exclusion thresholds are shown in Figures 3 and 4, with per-site and diagnosis-stratified visualizations provided in the Supplementary Materials.

Preprocessing Integrity Checks (fMRIPrep)

All preprocessing failures are logged, parsed, and categorized using custom scripts in `s7_fmriprep/`. Failure modes of fMRIPrep preprocessing include missing BOLD inputs, TemplateFlow binding issues, insufficient memory, FreeSurfer recon-all crashes, and susceptibility distortion correction failures. For syn-SDC failures caused by missing PhaseEncodingDirection metadata (predominantly in Philips scanners), sessions are reprocessed without distortion correction. These cases are explicitly flagged in the final dataset to allow stratified analyses or exclusion, if desired.

Final Inclusion Validation

The final dataset includes only sessions that pass all prior QC stages and meet additional stability criteria. These include having fewer than 30% censored frames ($FD > 0.5$ mm), at least 5 minutes of low-motion data, and site-specific acceptable Euler numbers. All inclusion/exclusion decisions are encoded in `included_sessions.tsv` and `excluded_sessions.tsv`, with standardized failure labels documenting the reason for exclusion. Summary counts across QC stages are reported in Table 4.

A)

Initial Session Count: 2893 (1153 subjects)

Phase	Parameter	Criteria	Rows Dropped	Remaining Rows
Phase 0	BIDS	Sessions flagged due to known errors in Clinica BIDS conversion.	0	2893
	Missing Data	Sessions where required NIfTI or JSON files are missing after Clinica conversion.	141	2752
	T1w Image Missing	Session does not have a T1-weighted image.	69	2683
Phase 1	ScanDepth (dim ₃ × pixdim ₃)	Scan Depth (dim ₃ × pixdim ₃) is outside the range [155, 180].	25	2658
	RepetitionTime (TR)	Sessions where TR falls outside [0.5–1.0] or [2.9–3.1] seconds.	27	2631
	Scan Duration	Sessions where total scan duration (TR × volumes) is less than 5 minutes.	7	2624
Phase 2	PercentPhaseFOV	A session with an unusually low value of ≤ 72.	1	2623
	CoilString	Sessions that use Q-BODY or BODY coils.	2	2621
TOTAL	—	—	272	2621

Final Session Count: 2621 (1105 subjects)

B)

Histogram of Sessions per Subject

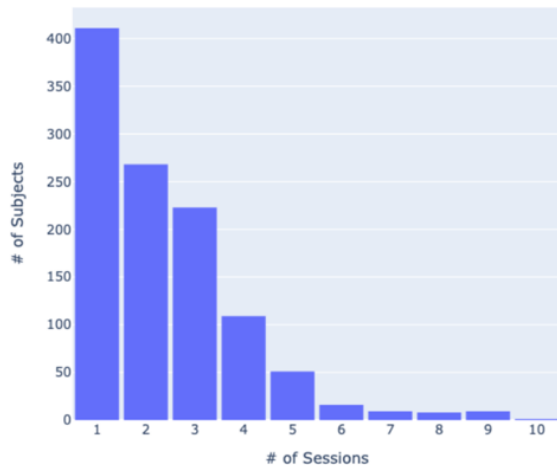


Figure 5. Example tables generated in the post_clinica_qc/main.ipynb notebook for inclusion/exclusion criteria based on Clinica/BIDS errors and scanner parameters. **A)** Summary table of criteria for excluding subjects and/or sessions in step 5. The number of subjects and sessions included/excluded at each stage is summarized. **B)** Histograms visualizing the number of sessions per subject after initial QC.

5 Usage Notes

The curated ADNI resting-state fMRI dataset produced by this protocol is intended as a high-quality, reproducible starting point for downstream neuroimaging, biomarker, and machine-learning analyses. Because ADNI data span multiple sites, scanner platforms, and acquisition protocols, careful consideration of QC outputs and metadata is essential when designing analyses. The following usage notes describe best practices for interpreting, integrating, and extending the dataset.

Interpreting the QC Outputs

After running the pipeline, the repository will contain machine-readable QC tables covering every stage of processing (Sections 2 and 3). We recommend beginning by examining: included_sessions.tsv: the final list of all subjects and sessions that passed all QC criteria, ii) excluded_sessions.tsv: sessions removed at any stage, with the specific exclusion reason, iii) motion_summary.tsv: mean framewise displacement, DVARS, percent scrubbed frames, iv) euler_summary.tsv: structural cortical surface quality (Euler number), and v) MRIQC outputs (iqm_merged.tsv, iqm_outliers.tsv): quantitative quality metrics for T1 and BOLD images. These tables allow users to evaluate data quality, verify reproducibility, adjust QC thresholds if desired, and determine the suitability of specific sessions or subgroups for further analysis.

Reproducing the Entire Pipeline

Users with ADNI access can fully reproduce this dataset through the following steps:

1. Clone the repository
2. Edit the configuration & environment files: config/config_adni.yaml & env/environment_adni.yaml
3. Ensure container runtimes (Apptainer) are installed
4. Download raw DICOMs and metadata via LONI
5. Run the scripts associated with each step
6. Inspect QC outputs in s5_post_clinica_qc/, s6_mriqc/, and s8_final_qc/
7. Use included_sessions.tsv as the analysis-ready dataset

Extending or Modifying the Pipeline

The modular structure of the workflow enables users to make modifications, for example: adjust MRIQC IQM thresholds, change the scanner parameter inclusion/exclusion heuristics, use alternative output spaces or fmriprep flags. Each step can be run independently, allowing partial re-processing without repeating the entire workflow.

Support and Troubleshooting

A comprehensive troubleshooting guide is provided in TROUBLESHOOTING.md, covering common ADNI DICOM issues, Clinica conversion failures, fMRIprep crashes and workarounds, HPC resource recommendations, and log-parsing tools for identifying failed subjects. Users are encouraged to submit issues via GitHub for additional support.

This workflow provides a transparent, reproducible, multi-level pipeline for preparing ADNI resting-state fMRI data. The accompanying QC outputs, configuration files, and containerized scripts enable researchers to reliably generate analysis-ready datasets that are robust to scanner variation and suitable for a broad range of neuroimaging applications.

6 Code Availability

All code required to reproduce the complete ADNI resting-state fMRI preprocessing workflow is openly available in the accompanying GitHub repository https://github.com/mandymejia/ADNI_fMRI_protocol. The repository includes:

- **Workflow orchestration files:**
 - A central configuration file (config/config_adni.yaml) specifying all paths, software versions, QC thresholds, and container locations
 - A Makefile defining all processing steps and dependencies
- **Step-by-step pipeline scripts** corresponding to this manuscript's Methods sections and GitHub folder structure:
 - s1_setup_account/: instructions for obtaining ADNI access
 - s2_download/: LONI download guidance
 - s3_organize/: DICOM organization and initial QC scripts
 - s4_clinica/: Clinica DICOM to BIDS conversion scripts and logs
 - s5_post_clinica_qc/: post-conversion QC scripts
 - s6_mriqc/: MRIQC execution, IQM extraction, and outlier-detection code
 - s7_fmriprep/: fMRIPrep preprocessing wrappers and log parsers
 - s8_final_qc/: integrated QC tools and final sample derivation
- **Containerized software environments:**
 - Apptainer/Singularity recipes and instructions for running MRIQC (v23.1.0) and fMRIPrep (25.2.3). These containers fully specify all software dependencies, ensuring reproducibility across computing environments and time.
- **Quality-control utilities and documentation:**
 - Scripts for motion QC, Euler number QC, MRIQC thresholding, session exclusion, and scanner/parameter summaries
 - TROUBLESHOOTING.md covering common ADNI-specific issues

All workflows and scripts are version controlled. A static, citable snapshot of the repository (including the Makefile, configuration files, QC code, and documentation) will be archived on Zenodo, and a DOI will be provided upon publication. This ensures that any

researcher with ADNI access can regenerate every derivative, QC table, and processing decision described in this manuscript.

7 Discussion and Impact

Resting-state fMRI provides a unique window into large-scale functional brain organization and has shown promise for detecting early network-level changes associated with cognitive decline and Alzheimer's disease. Despite this potential, ADNI rs-fMRI data have remained substantially underutilized relative to structural and PET imaging, largely due to the complexity of data curation, preprocessing, and quality control in a heterogeneous, multisite dataset.

This protocol directly addresses these barriers by providing a transparent, end-to-end framework for transforming raw ADNI rs-fMRI data into analysis-ready derivatives with fully documented quality-control decisions. By integrating clinical-imaging data alignment, standardized preprocessing, and multi-level QC into a single reproducible workflow, we lower the technical threshold required to use ADNI functional data at scale.

Importantly, this work enables a shift from small, selectively curated rs-fMRI samples toward large, harmonized cohorts suitable for biomarker discovery, longitudinal modeling, and machine learning. The resulting dataset makes it feasible to study functional connectivity changes across disease stages, evaluate fMRI-based prognostic markers, and integrate functional measures with existing structural, PET, and fluid biomarkers already widely used in ADNI research.

More broadly, this protocol serves as a template for curating legacy fMRI datasets collected before modern standards such as BIDS and fMRIprep were widely adopted. Many large clinical neuroimaging studies face similar challenges of heterogeneity, missing metadata, and inconsistent acquisition protocols. The strategies presented here, particularly upstream validation, conditional preprocessing, and transparent QC reporting, are broadly applicable beyond ADNI and can accelerate reuse of existing neuroimaging resources.

By making ADNI rs-fMRI data more accessible, reproducible, and interpretable, this work expands the scientific value of a major public resource and opens new opportunities for functional biomarker discovery in Alzheimer's disease and related neurodegenerative disorders.

References

Abraham, A., Pedregosa, F., Eickenberg, M., Gervais, P., Mueller, A., Kossaifi, J., Gramfort, A., Thirion, B., & Varoquaux, G. (2014). Machine learning for neuroimaging with scikit-learn. *Frontiers in Neuroinformatics*, 8.

<https://doi.org/10.3389/fninf.2014.00014>

Alzheimer's Disease Neuroimaging Initiative. (n.d.). *ADNI*. Retrieved January 20, 2026, from <https://adni-lde.loni.usc.edu/>

Atkinson, D., Hill, D. L. G., Stoyle, P. N. R., Summers, P. E., & Keevil, S. F. (1997). Automatic correction of motion artifacts in magnetic resonance images using an entropy focus criterion. *IEEE Transactions on Medical Imaging*, 16(6), 903–910.

<https://doi.org/10.1109/42.650886>

Avants, B. B., Epstein, C. L., Grossman, M., & Gee, J. C. (2008). Symmetric diffeomorphic image registration with cross-correlation: Evaluating automated labeling of elderly and neurodegenerative brain. *Medical Image Analysis*, 12(1), 26–41.

<https://doi.org/10.1016/j.media.2007.06.004>

Behzadi, Y., Restom, K., Liau, J., & Liu, T. T. (2007). A component based noise correction method (CompCor) for BOLD and perfusion based fMRI. *NeuroImage*, 37(1), 90–101.

<https://doi.org/10.1016/j.neuroimage.2007.04.042>

Ciric, R., Thompson, W. H., Lorenz, R., Goncalves, M., MacNicol, E., Markiewicz, C. J., Halchenko, Y. O., Ghosh, S. S., Gorgolewski, K. J., Poldrack, R. A., & Esteban, O. (2022). TemplateFlow: FAIR-sharing of multi-scale, multi-species brain models. *Nature Methods*, 19, 1568–1571. <https://doi.org/10.1038/s41592-022-01681-2>

Cox, R. W. (1996). AFNI: Software for analysis and visualization of functional magnetic resonance neuroimages. *Computers and Biomedical Research*, 29(3), 162–173.

Dale, A. M., Fischl, B., & Sereno, M. I. (1999). Cortical surface-based analysis. I. Segmentation and surface reconstruction. *Neuroimage*, 9(2), 179–194.

<https://doi.org/10.1006/nimg.1998.0395>

Esteban, O., Birman, D., Schaer, M., Koyejo, O. O., Poldrack, R. A., & Gorgolewski, K. J. (2017). MRIQC: Advancing the automatic prediction of image quality in MRI from unseen sites. *PLOS ONE*, 12(9), e0184661.

<https://doi.org/10.1371/journal.pone.0184661>

Esteban, O., Blair, R., Markiewicz, C. J., Berleant, S. L., Moodie, C., Ma, F., Isik, A. I., Erramuzpe, A., Kent, M., James D. and Goncalves, DuPre, E., Sitek, K. R., Gomez, D. E. P., Lurie, D. J., Ye, Z., Poldrack, R. A., & Gorgolewski, K. J. (2018). fMRIprep 25.2.3. Software. <https://doi.org/10.5281/zenodo.852659>

Esteban, O., Markiewicz, C. J., Blair, R. W., Moodie, C. A., Isik, A. I., Erramuzpe, A., Kent, J. D., Goncalves, M., DuPre, E., Snyder, M., Oya, H., Ghosh, S. S., Wright, J., Durnez, J., Poldrack, R. A., & Gorgolewski, K. J. (2018). fMRIprep: A robust preprocessing pipeline for functional MRI. *Nature Methods*, 1. <https://doi.org/10.1038/s41592-018-0235-4>

Evans, A., Janke, A., Collins, D., & Baillet, S. (2012). Brain templates and atlases. *Neuroimage*, 62(2), 911–922. <https://doi.org/10.1016/j.neuroimage.2012.01.024>

Fonov, V., Evans, A., McKinstry, R., Almlí, C., & Collins, D. (2009). Unbiased nonlinear average age-appropriate brain templates from birth to adulthood. *NeuroImage*, 47, S102. [https://doi.org/10.1016/S1053-8119\(09\)70884-5](https://doi.org/10.1016/S1053-8119(09)70884-5)

Friedman, L., Stern, H., Brown, G. G., Mathalon, D. H., Turner, J., Glover, G. H., Gollub, R. L., Lauriello, J., Lim, K. O., Cannon, T., Greve, D. N., Bockholt, H. J., Belger, A., Mueller, B., Doty, M. J., He, J., Wells, W., Smyth, P., Pieper, S., ... Potkin, S. G. (2008). Test-retest and between-site reliability in a multicenter fMRI study. *Human Brain Mapping*, 29(8), 958–972. <https://doi.org/10.1002/hbm.20440>

Ganzetti, M., Wenderoth, N., & Mantini, D. (2016). Intensity Inhomogeneity Correction of Structural MR Images: A Data-Driven Approach to Define Input Algorithm Parameters. *Frontiers in Neuroinformatics*, 10. <https://doi.org/10.3389/fninf.2016.00010>

Gau, R., Noble, S., Heuer, K., Bottenhorn, K. L., Bilgin, I. P., Yang, Y.-F., Huntenburg, J. M., Bayer, J. M. M., Bethlehem, R. A. I., Rhoads, S. A., Vogelbacher, C., Borghesani, V., Levitis, E., Wang, H.-T., Van Den Bossche, S., Kobeleva, X., Legarreta, J. H., Guay, S., Atay, S. M., ... Zuo, X.-N. (2021). Brainhack: Developing a culture of open, inclusive, community-driven neuroscience. *Neuron*, 109(11), 1769–1775. <https://doi.org/10.1016/j.neuron.2021.04.001>

Glasser, M. F., Sotiroopoulos, S. N., Wilson, J. A., Coalson, T. S., Fischl, B., Andersson, J. L., Xu, J., Jbabdi, S., Webster, M., Polimeni, J. R., Van Essen, D. C., & Jenkinson, M. (2013). The minimal preprocessing pipelines for the Human Connectome Project. *NeuroImage*, 80, 105–124. <https://doi.org/10.1016/j.neuroimage.2013.04.127>

Gorgolewski, K., Burns, C. D., Madison, C., Clark, D., Halchenko, Y. O., Waskom, M. L., & Ghosh, S. (2011). Nipype: A flexible, lightweight and extensible neuroimaging data processing framework in Python. *Frontiers in Neuroinformatics*, 5, 13.

<https://doi.org/10.3389/fninf.2011.00013>

Gorgolewski, K. J., Auer, T., Calhoun, V. D., Craddock, R. C., Das, S., Duff, E. P., Flandin, G., Ghosh, S. S., Glatard, T., Halchenko, Y. O., Handwerker, D. A., Hanke, M., Keator, D., Li, X., Michael, Z., Maumet, C., Nichols, B. N., Nichols, T. E., Pellman, J., ... Poldrack, R. A. (2016). The brain imaging data structure, a format for organizing and describing outputs of neuroimaging experiments. *Scientific Data*, 3, 160044.

<https://doi.org/10.1038/sdata.2016.44>

Gorgolewski, K. J., Esteban, O., Markiewicz, C. J., Ziegler, E., Ellis, D. G., Notter, M. P., Jarecka, D., Johnson, H., Burns, C., Manhães-Savio, A., Hamalainen, C., Yvernault, B., Salo, T., Jordan, K., Goncalves, M., Waskom, M., Clark, D., Wong, J., Loney, F., ... Ghosh, S. (2018). Nipype. *Software*. <https://doi.org/10.5281/zenodo.596855>

Greve, D. N., & Fischl, B. (2009). Accurate and robust brain image alignment using boundary-based registration. *NeuroImage*, 48(1), 63–72.

<https://doi.org/10.1016/j.neuroimage.2009.06.060>

Jenkinson, M., Bannister, P., Brady, M., & Smith, S. (2002a). Improved optimization for the robust and accurate linear registration and motion correction of brain images. *NeuroImage*, 17(2), 825–841.

Jenkinson, M., Bannister, P., Brady, M., & Smith, S. (2002b). Improved Optimization for the Robust and Accurate Linear Registration and Motion Correction of Brain Images.

NeuroImage, 17(2), 825–841. <https://doi.org/10.1006/nimg.2002.1132>

Kaufman, L., Kramer, D. M., Crooks, L. E., & Ortendahl, D. A. (1989). Measuring signal-to-noise ratios in MR imaging. *Radiology*, 173(1), 265–267.

<https://doi.org/10.1148/radiology.173.1.2781018>

Klapwijk, E. T., van de Kamp, F., van der Meulen, M., Peters, S., & Wierenga, L. M. (2019). Qoala-T: A supervised-learning tool for quality control of FreeSurfer segmented MRI data. *NeuroImage*, 189, 116–129. <https://doi.org/10.1016/j.neuroimage.2019.01.014>

Klein, A., Ghosh, S. S., Bao, F. S., Giard, J., Häme, Y., Stavsky, E., Lee, N., Rossa, B., Reuter, M., Neto, E. C., & Keshavan, A. (2017). Mindboggling morphometry of human brains. *PLOS Computational Biology*, 13(2), e1005350.

<https://doi.org/10.1371/journal.pcbi.1005350>

Magnotta, V. A., Friedman, L., & FIRST BIRN. (2006). Measurement of Signal-to-Noise and Contrast-to-Noise in the fBIRN Multicenter Imaging Study. *Journal of Digital Imaging*, 19(2), 140–147. <https://doi.org/10.1007/s10278-006-0264-x>

Nichols, T. E., Das, S., Eickhoff, S. B., Evans, A. C., Glatard, T., Hanke, M., Kriegeskorte, N., Milham, M. P., Poldrack, R. A., Poline, J.-B., Proal, E., Thirion, B., Van Essen, D. C., White, T., & Yeo, B. T. T. (2017). Best practices in data analysis and sharing in neuroimaging using MRI. *Nature Neuroscience*, 20(3), 299–303.

<https://doi.org/10.1038/nn.4500>

Parlak, F., Saluja, S. S., & Mejia, A. (2025). *Robust normality transformation for outlier detection in diverse distributions, with application to functional neuroimaging data* (No. arXiv:2505.11806). arXiv. <https://doi.org/10.48550/arXiv.2505.11806>

Patriat, R., Reynolds, R. C., & Birn, R. M. (2017). An improved model of motion-related signal changes in fMRI. *NeuroImage*, 144, Part A, 74–82.

<https://doi.org/10.1016/j.neuroimage.2016.08.051>

Petersen, R. C., Aisen, P. S., Beckett, L. A., Donohue, M. C., Gamst, A. C., Harvey, D. J., Jack, C. R., Jagust, W. J., Shaw, L. M., Toga, A. W., Trojanowski, J. Q., & Weiner, M. W. (2010). Alzheimer's Disease Neuroimaging Initiative (ADNI). *Neurology*, 74(3), 201–209. <https://doi.org/10.1212/WNL.0b013e3181cb3e25>

Power, J. D., Barnes, K. A., Snyder, A. Z., Schlaggar, B. L., & Petersen, S. E. (2012). Spurious but systematic correlations in functional connectivity MRI networks arise from subject motion. *NeuroImage*, 59(3), 2142–2154.

<https://doi.org/10.1016/j.neuroimage.2011.10.018>

Power, J. D., Mitra, A., Laumann, T. O., Snyder, A. Z., Schlaggar, B. L., & Petersen, S. E. (2014). Methods to detect, characterize, and remove motion artifact in resting state fMRI. *NeuroImage*, 84(Supplement C), 320–341.

<https://doi.org/10.1016/j.neuroimage.2013.08.048>

Rosen, A. F. G., Roalf, D. R., Ruparel, K., Blake, J., Seelaus, K., Villa, L. P., Cricic, R., Cook, P. A., Davatzikos, C., Elliott, M. A., de La Garza, A. G., Gennatas, E. D., Quarmley, M., Schmitt, J. E., Shinohara, R. T., Tisdall, M. D., Craddock, R. C., Gur, R. E., Gur, R. C., &

Satterthwaite, T. D. (2018). Quantitative Assessment of Structural Image Quality. *NeuroImage*, 169, 407–418. <https://doi.org/10.1016/j.neuroimage.2017.12.059>

Routier, A., Burgos, N., Díaz, M., Bacci, M., Bottani, S., El-Rifai, O., Fontanella, S., Gori, P., Guillou, J., Guyot, A., Hassanaly, R., Jacquemont, T., Lu, P., Marcoux, A., Moreau, T., Samper-González, J., Teichmann, M., Thibeau-Sutre, E., Vaillant, G., ... Colliot, O. (2021). Clinica: An Open-Source Software Platform for Reproducible Clinical Neuroscience Studies. *Frontiers in Neuroinformatics*, 15. <https://doi.org/10.3389/fninf.2021.689675>

Samper-González, J., Burgos, N., Bottani, S., Fontanella, S., Lu, P., Marcoux, A., Routier, A., Guillou, J., Bacci, M., Wen, J., Bertrand, A., Bertin, H., Habert, M.-O., Durrelman, S., Evgeniou, T., & Colliot, O. (2018). Reproducible evaluation of classification methods in Alzheimer's disease: Framework and application to MRI and PET data. *NeuroImage*, 183, 504–521. <https://doi.org/10.1016/j.neuroimage.2018.08.042>

Satterthwaite, T. D., Elliott, M. A., Gerraty, R. T., Ruparel, K., Loughead, J., Calkins, M. E., Eickhoff, S. B., Hakonarson, H., Gur, R. C., Gur, R. E., & Wolf, D. H. (2013). An improved framework for confound regression and filtering for control of motion artifact in the preprocessing of resting-state functional connectivity data. *NeuroImage*, 64(1), 240–256. <https://doi.org/10.1016/j.neuroimage.2012.08.052>

Toga, A. W., Neu, S., Sheehan, S. T., Crawford, K., & Initiative, for the A. D. N. (2024). The informatics of ADNI. *Alzheimer's & Dementia*, 20(10), 7320–7330. <https://doi.org/10.1002/alz.14099>

Tustison, N. J., Avants, B. B., Cook, P. A., Zheng, Y., Egan, A., Yushkevich, P. A., & Gee, J. C. (2010). N4ITK: Improved N3 Bias Correction. *IEEE Transactions on Medical Imaging*, 29(6), 1310–1320. <https://doi.org/10.1109/TMI.2010.2046908>

Weiner, M. W., Kanoria, S., Miller, M. J., Aisen, P. S., Beckett, L. A., Conti, C., Diaz, A., Flenniken, D., Green, R. C., Harvey, D. J., Jack, C. R., Jagust, W., Lee, E. B., Morris, J. C., Nho, K., Nosheny, R., Okonkwo, O. C., Perrin, R. J., Petersen, R. C., ... Veitch, D. P. (2024). Overview of Alzheimer's Disease Neuroimaging Initiative and future clinical trials. *Alzheimer's & Dementia*, 21(1), e14321. <https://doi.org/10.1002/alz.14321>

Weiner, M. W., Kanoria, S., Miller, M. J., Aisen, P. S., Beckett, L. A., Conti, C., Diaz, A., Flenniken, D., Green, R. C., Harvey, D. J., Jack Jr., C. R., Jagust, W., Lee, E. B., Morris, J. C., Nho, K., Nosheny, R., Okonkwo, O. C., Perrin, R. J., Petersen, R. C., ... Initiative, for the A. D. N. (2025). Overview of Alzheimer's Disease Neuroimaging Initiative and future clinical trials. *Alzheimer's & Dementia*, 21(1), e14321.

<https://doi.org/10.1002/alz.14321>

Weiner, M. W., Veitch, D. P., Aisen, P. S., Beckett, L. A., Cairns, N. J., Cedarbaum, J., Green, R. C., Harvey, D., Jack, C. R., Jagust, W., Luthman, J., Morris, J. C., Petersen, R. C., Saykin, A. J., Shaw, L., Shen, L., Schwarz, A., Toga, A. W., Trojanowski, J. Q., & Initiative, A. D. N. (2015). 2014 Update of the Alzheimer's Disease Neuroimaging Initiative: A review of papers published since its inception. *Alzheimer's & Dementia*, 11(6), e1–e120. <https://doi.org/10.1016/j.jalz.2014.11.001>

Weiner, M. W., Veitch, D. P., Aisen, P. S., Beckett, L. A., Cairns, N. J., Green, R. C., Harvey, D., Jack, C. R., Jagust, W., Liu, E., Morris, J. C., Petersen, R. C., Saykin, A. J., Schmidt,

M. E., Shaw, L., Shen, L., Siuciak, J. A., Soares, H., Toga, A. W., ... Initiative, A. D. N.

(2013). The Alzheimer's Disease Neuroimaging Initiative: A review of papers

published since its inception. *Alzheimer's & Dementia*, 9(5), e111–e194.

<https://doi.org/10.1016/j.jalz.2013.05.1769>

Weiner, M. W., Veitch, D. P., Aisen, P. S., Beckett, L. A., Cairns, N. J., Green, R. C., Harvey,

D., Jack, C. R., Jagust, W., Liu, E., Morris, J. C., Petersen, R. C., Saykin, A. J., Schmidt,

M. E., Shaw, L., Siuciak, J. A., Soares, H., Toga, A. W., Trojanowski, J. Q., & Initiative,

A. D. N. (2012). The Alzheimer's Disease Neuroimaging Initiative: A review of papers

published since its inception. *Alzheimer's & Dementia*, 8(1S), S1–S68.

<https://doi.org/10.1016/j.jalz.2011.09.172>

Yao, X., Yan, J., Ginda, M., Börner, K., Saykin, A. J., Shen, L., & Initiative, for the A. D. N.

(2017). Mapping longitudinal scientific progress, collaboration and impact of the

Alzheimer's disease neuroimaging initiative. *PLOS ONE*, 12(11), e0186095.

<https://doi.org/10.1371/journal.pone.0186095>

Zhang, Y., Brady, M., & Smith, S. (2001). Segmentation of brain MR images through a hidden

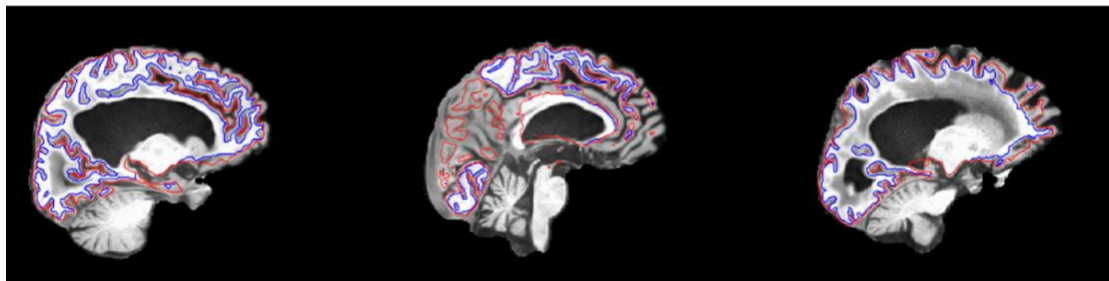
Markov random field model and the expectation-maximization algorithm. *IEEE*

Transactions on Medical Imaging, 20(1), 45–57. <https://doi.org/10.1109/42.906424>

Supplemental Figures

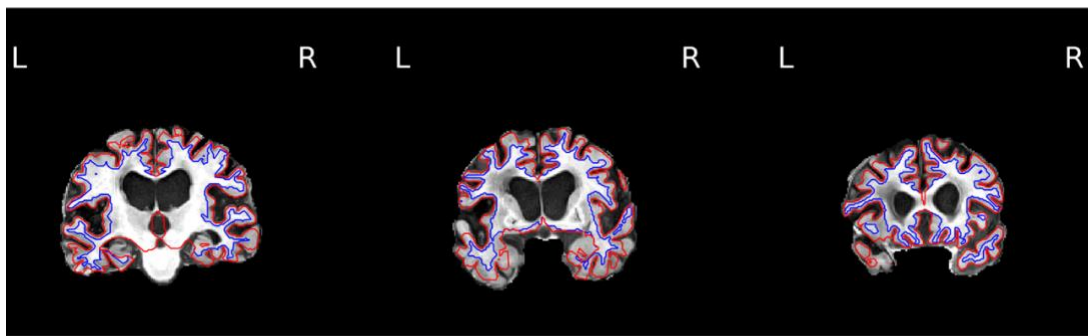
CNR outlier

sub-ADNI114S6347_ses-M024



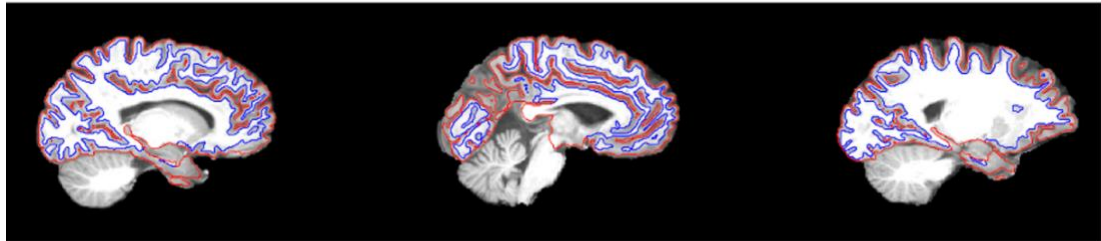
CJV outliers

sub-ADNI126S6559_ses-M036



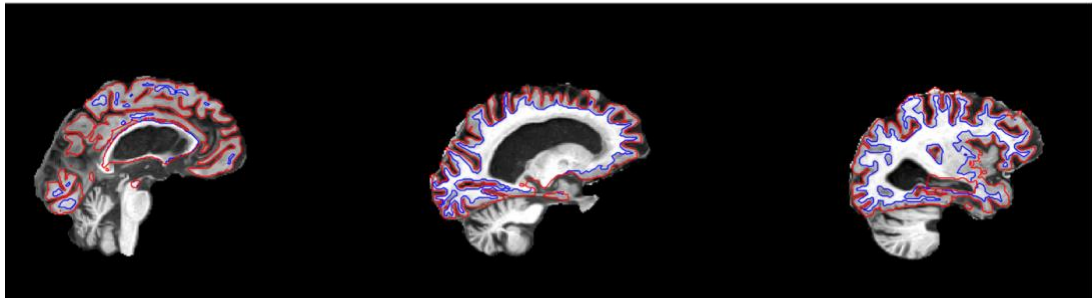
FWHM outlier

sub-ADNI131S6170_ses-M042



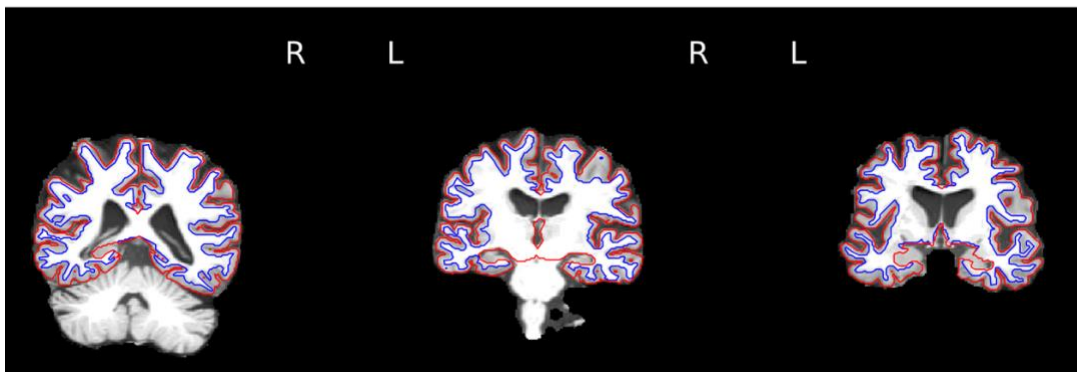
SNR outlier

sub-ADNI099S4086_ses-M078



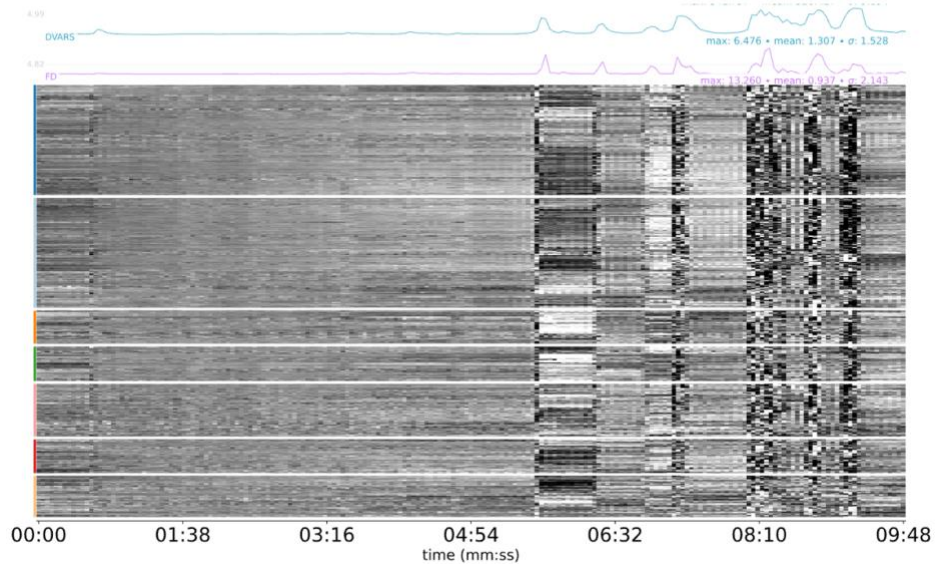
TPM outliers

sub-ADNI1002S4219_ses-M012



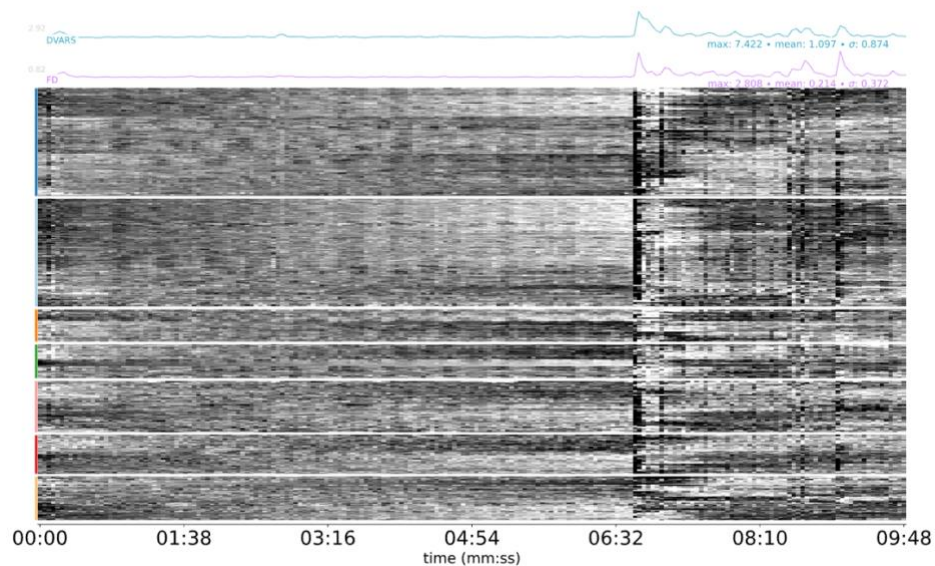
AOR outlier

sub-ADNI1035S7021_ses-M000



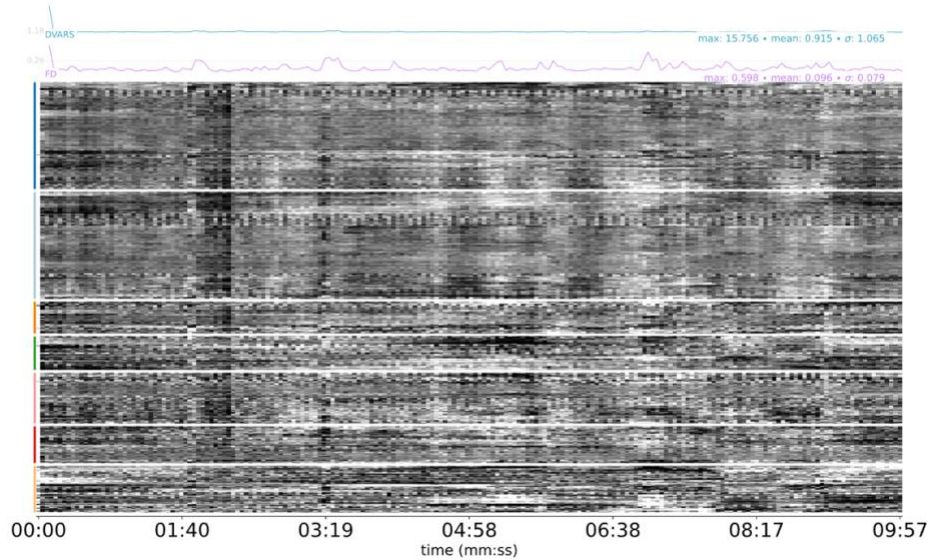
AQI outlier

sub-ADNI020S6513_ses-M012

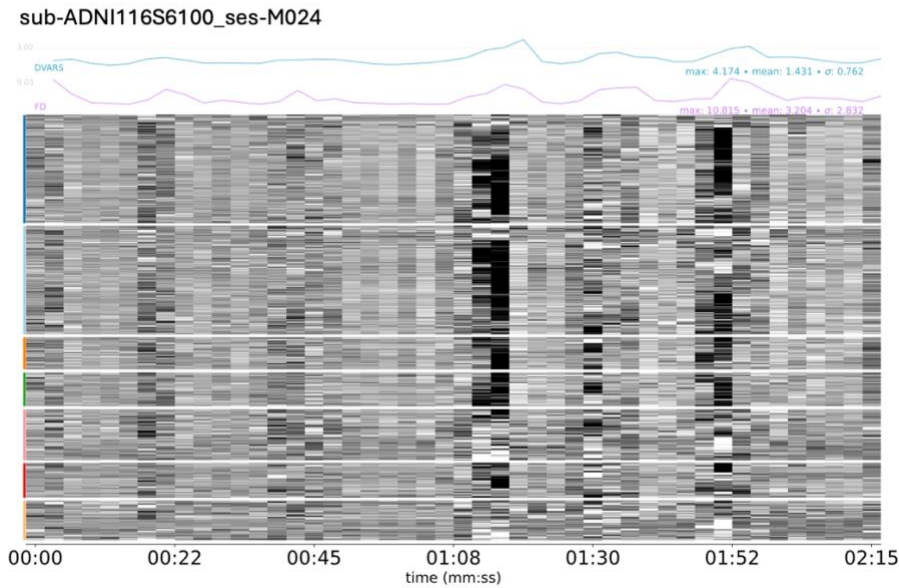


FWHM outlier

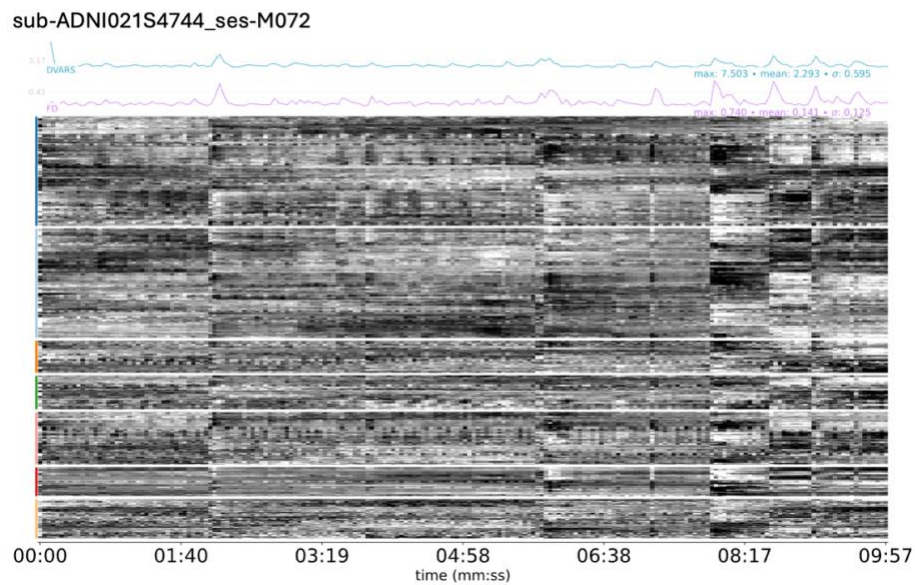
sub-ADNI127S6433_ses-M000



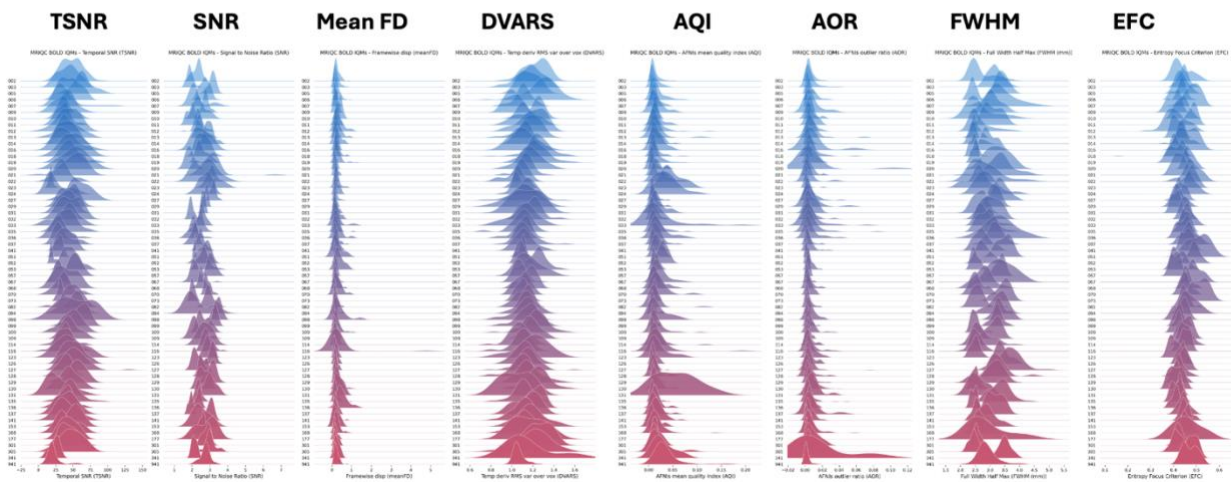
meanFD outlier



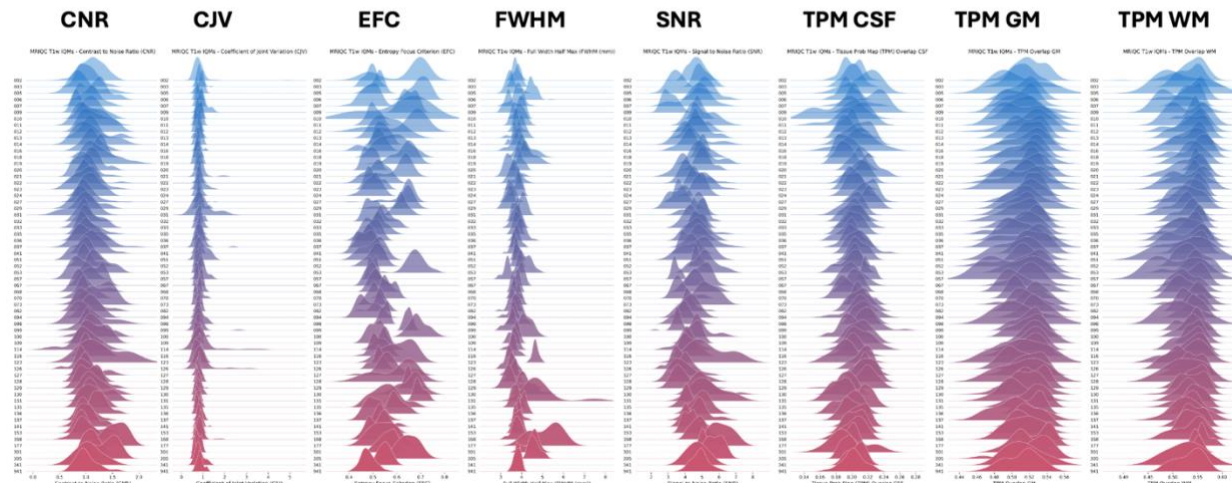
TSNR outlier

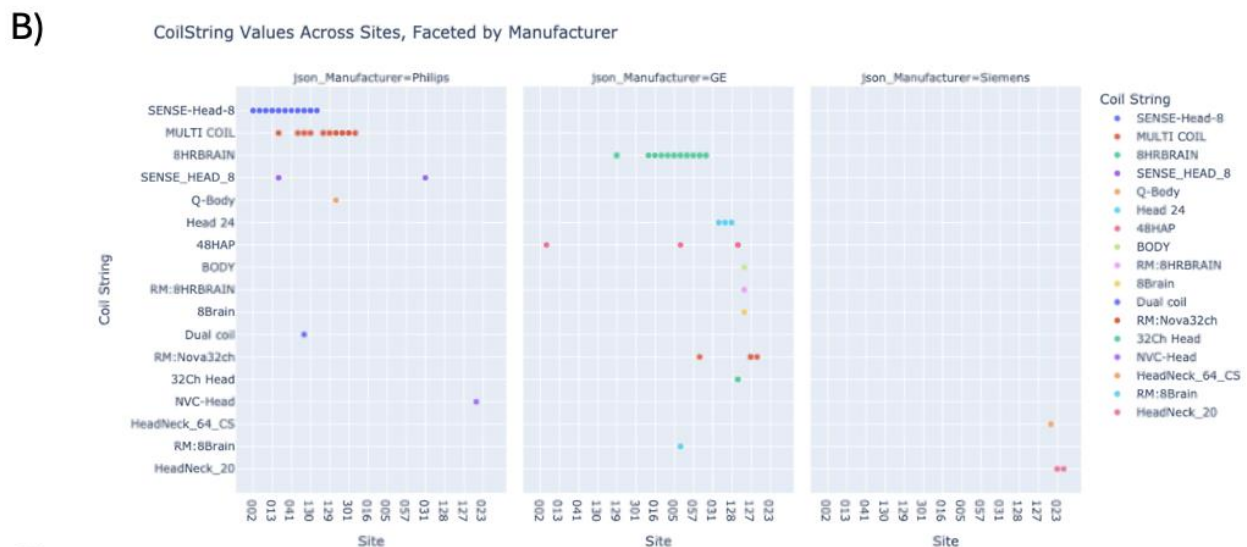


fMRI BOLD
IQMs
by site



T1w
IQMs
by site





C) Final Missing Data by Parameter (Faceted by Manufacturer)

Parameter	Philips	Siemens	GE
RepetitionTime	0	0	0
MagneticFieldStrength	0	0	0
ManufacturersModelName	0	0	0
InstitutionName	0	63	0
MRAcquisitionType	0	0	0
SliceThickness	0	0	0
SpacingBetweenSlices	0	0	0
EchoTime	0	0	0
FlipAngle	0	0	0
PercentPhaseFOV	0	0	0
PercentSampling	0	0	0
EchoTrainLength	0	220	524
AcquisitionMatrixPE	0	16	0
PhaseEncodingDirection	899	30	10
CoilString	0	1181	0
MRAcquisitionFrequencyEncodingSteps	779	1196	524
PhaseEncodingAxis	0	1167	514
ScanDepth	0	0	0

Figure 5. Example of scanner parameters (y-axis) visualized across manufacturers (facets) and sites (x-axis). Here we show two example parameters, **A**) Total scan duration and **B**) CoilString. All other scanner parameters are visualized in the same manner, and these plots (and code for generating them) are in the GitHub (post_clinica_qc/analysis/create_report/main.ipynb). **C**) Table summarizing the per-scanner manufacturer missing scanner parameters.

Supplemental Text

FMRIPrep preprocessing methods

Anatomical preprocessing

The T1 image for each subject is corrected for intensity non-uniformity (INU) with N4BiasFieldCorrection (Tustison et al., 2010), distributed with ANTs 2.6.2 (Avants et al., 2008), and used as T1 reference throughout the workflow. The T1 reference is then skull-stripped with a Nipype implementation of the antsBrainExtraction.sh workflow (from ANTs), using OASIS30ANTs as target template. Brain tissue segmentation of cerebrospinal fluid (CSF), white-matter (WM) and gray-matter (GM) is performed on the brain-extracted T1 using FSL fast (Zhang et al., 2001). Brain surfaces are reconstructed using recon-all (FreeSurfer 7.3.2) (Dale et al., 1999), and the brain mask estimated previously is refined with a custom variation of the method to reconcile ANTs-derived and FreeSurfer-derived segmentations of the cortical gray-matter of Mindboggle (Klein et al., 2017). A FLAIR image is used to improve pial surface refinement. Brain surfaces are reconstructed using recon-all (FreeSurfer 7.3.2) (Dale et al., 1999), and the brain mask estimated previously was refined with a custom variation of the method to reconcile ANTs-derived and FreeSurfer-derived segmentations of the cortical gray-matter of Mindboggle (Klein et al., 2017). Volume-based spatial normalization to two standard spaces (MNI152NLin6Asym, MNI152NLin2009cAsym) is performed through nonlinear registration with antsRegistration (ANTs 2.6.2), using brain-extracted versions of both T1 reference and the T1 template. The following templates were selected for spatial normalization and accessed with TemplateFlow (Ciric et al., 2022) (25.0.4): FSL's MNI ICBM 152 non-linear 6th Generation Asymmetric Average Brain Stereotaxic Registration Model (Evans et al., 2012) [TemplateFlow ID: MNI152NLin6Asym], ICBM 152 Nonlinear Asymmetrical template version 2009c (Fonov et al., 2009) [TemplateFlow ID: MNI152NLin2009cAsym].

Functional preprocessing

First, a BOLD reference volume is generated for use in head motion correction. Head-motion parameters with respect to the BOLD reference (transformation matrices, and six corresponding rotation and translation parameters) are estimated before spatiotemporal filtering using FSL mcflirt (Jenkinson et al., 2002a). The BOLD reference is then co-registered to the T1 reference using bbregister (FreeSurfer), which implements boundary-based registration (Greve & Fischl, 2009). Co-registration is configured with six degrees of freedom.

Several confounding time series are calculated based on the preprocessed BOLD: framewise displacement (FD), DVARS, and three region-wise global signals. FD is computed using two formulations: the Power formulation (absolute sum of relative motions) (Power et al., 2014) and the Jenkinson formulation (relative root-mean-square displacement between affines) (Jenkinson et al., 2002b). FD and DVARS are calculated for each functional run, both using their implementations in Nipype (following the definitions by Power (Power et al., 2014)). The three global signals are extracted within the CSF, the WM, and the whole-brain masks.

Additionally, a set of physiological regressors are extracted to allow for component-based noise correction (CompCor (Behzadi et al., 2007)). Principal components are estimated after high-pass filtering the preprocessed BOLD time series (using a discrete cosine filter with 128s cut-off) for the two CompCor variants: temporal (tCompCor) and anatomical (aCompCor). tCompCor components were calculated from the top 2% variable voxels within the brain mask. For aCompCor, three probabilistic masks (CSF, WM and combined CSF+WM) are generated in anatomical space. The implementation in fMRIprep differs from that of Behzadi et al. (Behzadi et al., 2007) in that, instead of eroding the masks by 2 pixels on BOLD space, a mask of pixels that likely contain a volume fraction of GM is removed from the WM and CSF masks. This mask is obtained by dilating a GM mask extracted from the FreeSurfer's aseg segmentation, and it ensures components are not extracted from voxels containing a pre-set minimal fraction of GM. Finally, these masks are resampled into BOLD space and binarized by thresholding at 0.99 (as in the original implementation). Components are also calculated separately within the WM and CSF masks. For each CompCor decomposition, the k components with the largest singular values are retained, such that the retained components' time series are sufficient to explain 50 percent of the variance across the nuisance mask. The remaining components are dropped from consideration.

The head-motion estimates calculated in the correction step are also placed within the corresponding confounds file. The confound time series derived from head motion estimates and global signals are expanded with the inclusion of temporal derivatives and quadratic terms for each (Satterthwaite et al., 2013). Frames that exceed a threshold of 0.5

mm FD or 1.5 standardized DVARS are annotated as motion outliers. Additional nuisance timeseries are calculated by means of principal components analysis of the signal found within a thin band (crown) of voxels around the edge of the brain, as proposed by Patriat et al. (Patriat et al., 2017).

The BOLD time series are resampled onto the following surfaces (Freesurfer reconstruction nomenclature): fsnative, fsaverage5, fsLR. The BOLD time series are resampled from T1 native (subject-specific) volumetric space into surface native (subject-specific) space, and then the surface native mesh is resampled onto the left/right-symmetric group-level template "fsLR" using the Connectome Workbench (Glasser et al., 2013). Grayordinates files (Glasser et al., 2013) containing 91k cortical and subcortical coordinates are also generated with surface data transformed directly to fsLR space and subcortical data transformed to 2 mm resolution MNI152NLin6Asym space. All resamplings can be performed with a single interpolation step by composing all the pertinent transformations (i.e., head-motion transform matrices, susceptibility distortion correction when available, and co-registrations to anatomical and output spaces). Gridded (volumetric) resamplings are performed using nitransforms, configured with cubic B-spline interpolation. Non-gridded (surface) resamplings are performed using mri_vol2surf (Freesurfer).

ADNI specific fMRIPrep preprocessing errors

Missing BOLD file errors occur when subjects have multiple session directories but only a subset contain functional data (e.g., ses-M000/, ses-M006/, ses-M012/, ses-M048/, ses-M096/, with BOLD present only in later sessions). To prevent fMRIPrep failures in these cases, the pipeline explicitly inspects session directories prior to submission and dynamically restricts fMRIPrep execution to sessions that contain valid BOLD files. As a result, fMRIPrep jobs are only launched for subject–session pairs that meet minimum data requirements. This logic is implemented in the s7_fmriprep/fMRIPrep_rerun_array.slurm script and is applied uniformly across all subjects.

TemplateFlow binding and memory-related errors affect only three subjects in our data download. These errors are resolved by adjusting resource allocation and ensuring that the TemplateFlow directory is correctly mounted inside the container. The provided fMRIPrep execution scripts automatically download and bind the TemplateFlow directory, allowing these cases to be successfully reprocessed without further intervention.

FreeSurfer recon-all failures reflect unrecoverable errors in cortical surface reconstruction, most likely due to low-quality anatomical data. Subjects with these

failures are excluded from downstream analyses, as these errors cannot be reliably corrected.

Syn-sdc failures are caused by missing or invalid PhaseEncodingDirection metadata in the BOLD JSON files, which is common for certain ADNI acquisitions (primarily from Philips scanners). Because PhaseEncodingDirection is required for fieldmap-less distortion correction, these runs fail when syn-sdc is enabled. Our error classification automatically detects this condition (`find_syn_pedir_failures.py`) and re-runs affected subjects without the `--use-syn-sdc` flag using `s7_fmriprep/fMRIPrep_rerun_synflag_array.slurm`. Users may choose to exclude these subjects due to these differences in preprocessing; however, we retain them in the final dataset, as ADNI already contains unavoidable heterogeneity in acquisition parameters and available anatomical images (e.g., presence or absence of T2 scans).

Records Produced at Each Step

Steps 1–2: Data Acquisition Records

Folders: `s1_setup_account/`, `s2_download/`

These folders contain procedural guides (`s1_setup_account/README.md` & `s2_download/README.md`) but no data or scripts. Users must follow the instructions to setup their account and DUA, then download: i) DICOM ZIP archives, ii) metadata spreadsheets (e.g., ADNIMERGE, scanner protocols, QC files), iii) clinical and behavioral files, iv) image collection CSV files (describing DICOM directories of your image collection).

Step 3: DICOM Organization and Initial QC Records

Folder: `s3_organize/`

Generated records include:

- `dicom_dirs.csv`: a complete list of downloaded subjects and sessions
- `clinica_subs.txt`: a subject list to pass onto Clinica.

These records establish the ground truth of the raw imaging dataset and are essential for troubleshooting missing sessions or discrepancies between ADNI and local storage.

Step 4: BIDS Records and Clinica Metadata

Folder: s4_clinica/

Generated records include:

- BIDS directory (sub-*/ses-*) with .nii.gz and .json files
- participants.tsv: includes participant_id, sex, education, baseline age, ethnicity, site, baseline diagnosis, and baseline cognitive test scores.
- clinical_data.tsv: subject and session-specific clinical data matched to imaging sessions.
- dataset_description.json: contains the dataset name and BIDS version.
- fmri_paths.tsv, flair_paths.tsv, t1_paths.tsv: contains the mapping between DICOM directories and BIDS NIfTI files, associated metadata extracted from the DICOMS.
- clinica_conversion.logs: full record of conversion steps, including errors.

These records ensure traceability of every conversion decision and document known ADNI inconsistencies.

Step 5: Post-Clinica QC Records

Folder: s5_post_clinica_qc/

Generated records include:

- anchor_df.csv, anchor_plus_dicom.csv, anchor_plus_dicom_nifti_struct.csv: files providing links between BOLD and T1 DICOMS and NIfTI files, and additional scanner parameters. Image_ID, Series_ID, and Scan_Date are included in these files.
- missing_data.tsv: subjects that are missing NIfTI or JSON files after Clinica conversion.
- missing_T1.tsv: subjects that are missing T1 data but have a BOLD image. These subjects are manually checked (if you wish). Some can be recovered by manually running dcm2niix yourself (not using clinica).
- final_heuristics.tsv: subject list passed on to mriqc. One row per subject and per session.
- fmriprep_subjects.tsv: subject list passed on to fmriprep. Format is one row per subject, and sessions are stored as columns.

- tables and plots generated in main.ipynb: scanner parameters visualized across sites and manufacturers, tables summarizing the reasons subjects/sessions are excluded, and the number of included subjects after each heuristic.

These files document structural and temporal acquisition differences across ADNI sites and serve as the first round of exclusion.

Step 6: MRIQC Records

Folder: s6_mriqc/

Generated records include:

- Per-run JSON + TSV IQM files (subjects' quality metrics)
- Participant-level HTML reports
- Group-level HTML reports (BOLD/T1 summaries)
- Group-level TSV of all subjects' IQMs (group_bold.tsv, group_t1.tsv)
- T1_IQMs_rainclouds.pdf: visualization of all T1 IQMs, including the outlier threshold (Figure 2).
- BOLD_IQMs_rainclouds.pdf: visualization of all BOLD IQMs, including the outlier threshold (Figure 3).
- All_IQMs_with_QC_flags_clean.tsv: T1 and BOLD IQMs merged into a single file with columns for include/exclude based on outlier thresholds.

Because IQM logic is often opaque to end users, all intermediate tables and scripts are included to ensure full transparency.

Step 7: fMRIprep Records

Folder: s7_fmriprep/

Generated records include:

- BIDS-Derivatives compliant preprocessed data
- confounds_timeseries.tsv files
- MNI volumetric space outputs
- Surface outputs (fsnative, fsaverage:den-10k)
- Grayordinates CIFTI files (fsLR:den-91k)
- log_*.err & log_*.out: per-subject output and error logs
- fmriprep_error_report_ALL.csv: automated error summaries

Step 8: Final QC and Curated Dataset Records

Folder: s8_final_qc/

Generated records include:

- included_sessions.tsv: sessions meeting all criteria
- excluded_sessions.tsv: sessions removed with coded reasons
- euler_summary.tsv: sessions left and right hemisphere euler number and average euler number, site column (used to calculate site specific euler exclusion).
- motion_summary.tsv: one row per subject, summary of subject's motion parameters (meanFD, percent scrubbed, good_time, DVARS)
- motion_timeseries.tsv: one row per volume per session, per subject motion parameters.

These records define the final reproducible sample for downstream analyses.